



Conditional Deletion of Activating Rearranged During Transfection Receptor Tyrosine Kinase Leads to Impairment of Photoreceptor Ribbon Synapses and Disrupted Visual Function in Mice

OPEN ACCESS

Edited by:

Jianhai Du,
West Virginia University, United States

Reviewed by:

Wallace B. Thoreson,
University of Nebraska Medical
Center, United States
Yoshihiko Tsukamoto,
Hyogo College of Medicine, Japan

***Correspondence:**

Chung-Liang Chien
chien@ntu.edu.tw
Nan-Kai Wang
nw2189@cumc.columbia.edu

† These authors have contributed
equally to this work

Specialty section:

This article was submitted to
Neurodegeneration,
a section of the journal
Frontiers in Neuroscience

Received: 30 June 2021

Accepted: 11 October 2021

Published: 05 November 2021

Citation:

Peng W-H, Liao M-L, Huang W-C,
Liu P-K, Levi SR, Tseng Y-J, Lee C-Y,
Yeh L-K, Chen K-J, Chien C-L and
Wang N-K (2021) Conditional Deletion
of Activating Rearranged During
Transfection Receptor Tyrosine Kinase
Leads to Impairment
of Photoreceptor Ribbon Synapses
and Disrupted Visual Function
in Mice. *Front. Neurosci.* 15:728905.
doi: 10.3389/fnins.2021.728905

Wei-Hao Peng¹, Meng-Lin Liao², Wan-Chun Huang², Pei-Kang Liu^{3,4,5,6}, Sarah R. Levi⁶, Yun-Ju Tseng⁶, Chia-Ying Lee⁷, Lung-Kun Yeh^{7,8}, Kuan-Jen Chen^{7,8}, Chung-Liang Chien^{2*†} and Nan-Kai Wang^{6*†}

¹ School of Medicine for International Students, College of Medicine, I-Shou University, Kaohsiung, Taiwan, ² Department of Anatomy and Cell Biology, College of Medicine, National Taiwan University, Taipei, Taiwan, ³ Department of Ophthalmology, Kaohsiung Medical University Hospital, Kaohsiung Medical University, Kaohsiung, Taiwan, ⁴ School of Medicine, College of Medicine, Kaohsiung Medical University, Kaohsiung, Taiwan, ⁵ Institute of Biomedical Sciences, National Sun Yat-sen University, Kaohsiung, Taiwan, ⁶ Department of Ophthalmology, Edward S. Harkness Eye Institute, Columbia University Irving Medical Center, Columbia University, New York, NY, United States, ⁷ Department of Ophthalmology, Chang Gung Memorial Hospital, Taoyuan, Taiwan, ⁸ College of Medicine, Chang Gung University, Taoyuan, Taiwan

Purpose: The rearranged during transfection (RET) receptor tyrosine kinase plays a key role in transducing signals related to cell growth and differentiation. *Ret* mutant mice show abnormal retinal activity and abnormal levels and morphology of bipolar cells, yet die on the 21st day after birth as a result of renal underdevelopment. To extend the observation period, we generated the *Ret* conditional knockout *Chx10-Cre;C-Ret^{flx/flx}* mouse model and analyzed the retinal function and morphological changes in mature and aging *Chx10-Cre;C-Ret^{flx/flx}* mice.

Methods: Retina-specific depletion of *Ret* was achieved using mice with floxed alleles of the *Ret* gene with CHX10-driven Cre recombinase; floxed mice without Cre expression were used as controls. Retinal function was examined using electroretinography (ERG), and 2-, 4-, 12-, and 24-month-old mice were analyzed by hematoxylin staining and immunohistochemistry to evaluate retinal morphological alterations. The ultrastructure of photoreceptor synapses was evaluated using electron microscopy.

Results: The results of the ERG testing showed that b-wave amplitudes were reduced in *Chx10-Cre;C-Ret^{flx/flx}* mice, whereas a-waves were not affected. A histopathological analysis revealed a thinner and disorganized outer plexiform layer at the ages of 12 and 24 months in *Chx10-Cre;C-Ret^{flx/flx}* mice. Moreover, the data provided by immunohistochemistry showed defects in the synapses of photoreceptor cells. This

result was confirmed at the ultrastructural level, thus supporting the participation of *Ret* in the morphological changes of the synaptic ribbon.

Conclusion: Our results provide evidence of the role of *Ret* in maintaining the function of the retina, which was essential for preserving the structure of the synaptic ribbon and supporting the integrity of the outer plexiform layer.

Keywords: GDNF family of ligands (GFL), rearranged during transfection (RET), mouse retina, ribbon synapses, Cre-loxP knockout mice

INTRODUCTION

The retina receives light signals at levels that span several orders of magnitude. Adaptive changes to different light levels occur at multiple sites within the retinal signal transmission and act together in processing the light information. In contrast to conventional neurons, photoreceptors do not signal via action potentials; rather, they continuously translate light into a graded transmitter release, with the highest exocytosis rates in the dark. To accomplish this task, photoreceptors and retinal bipolar cells contain a specialized type of synapse, the so-called ribbon synapse. The ribbon synapse is a specialized synaptic structure located in the outer plexiform layer (OPL) of the retina in which a synaptic “triad” is formed between the axonal pedicles of rods and cones and the dendrites of horizontal and bipolar cells. Through this special synapse, visual signals are transmitted from photoreceptors to bipolar and horizontal cells (Heidelberger et al., 2005). Morphologically, ribbon synapses are anchored to the plasma membrane in close vicinity to voltage-gated Ca^{2+} channels and are typically surrounded by a large number of synaptic vesicles (Sterling and Matthews, 2005). A previous study showed that the lack of active-zone-anchored synaptic ribbons reduced the presynaptic readily releasable vesicle pool and impaired synchronous visual signaling, thus affecting visual function (LoGiudice and Matthews, 2009). Therefore, photoreceptor ribbon synapses play an important role in visual function.

To protect central nervous system (CNS) cells, mutation-independent neuroprotective strategies—such as the glial-cell-line-derived neurotrophic factor (GDNF), the brain-derived neurotrophic factor (BDNF), the nerve growth factor (NGF), and the ciliary neurotrophic factor (CNTF)—have been applied to, and their therapeutic potential has been demonstrated in, the management of retinal impairment in various animal models (Chinskey et al., 2014). GDNF is a distant member of the transforming growth factor β (TGF- β) superfamily and a founder protein of the GDNF-family ligands (GFLs), which include neurturin (NRTN), artemin (ARTN), and persephin (PSPN) (Airaksinen and Saarma, 2002). All four GFLs (GDNF, NRTN, ARTN, and PSPN) signal via

the activation of the rearranged during transfection (RET) receptor tyrosine kinase, a single-pass transmembrane protein that contains four cadherin-like repeats in the extracellular domain and a typical intracellular tyrosine kinase domain (Durbec et al., 1996). These GFLs promote the survival of various neurons, including peripheral neurons and central motor and dopamine neurons, and have been suggested as candidate therapeutic agents for neurodegenerative diseases (Takahashi, 2001).

The function of GDNF in the nervous system has been investigated in many studies. GDNF promotes the differentiation and survival of rat midbrain dopamine neurons and increases the outgrowth of neurites and dopamine uptake *in vitro* (Lin et al., 1993). Moreover, GDNF stimulates the formation of new axon terminals in dopamine neurons, which has led to an increased interest in the therapeutic potential of GDNF for the management of Parkinson’s disease (Bourque and Trudeau, 2000). In addition, a previous study showed that GDNF supports the survival of spinal motoneurons (Henderson et al., 1994). In the eye, GDNF is mainly expressed in the retina and has potential therapeutic value by providing neuroprotection in the context of retinal degeneration (Koeberle and Ball, 1998). Moreover, GDNF was reported to be able to rescue retinal ganglion cells after axotomy (Yan et al., 1999) and to be very effective in retarding photoreceptor degeneration in the retinal degeneration 1 (*rd1*) mouse model (Frasson et al., 1999). Subretinal injection of GDNF decreased the loss of photoreceptors and provided a significant functional rescue, as demonstrated by recordable electroretinography (ERG) (Frasson et al., 1999). These studies suggest that GDNF-mediated RET signaling affects retinal function.

GDNF was shown to be a RET ligand, and extensive studies of intracellular signaling through RET have been performed. Specifically, mice carrying loss-of-function mutations in a variety of GFLs or in their receptors exhibited either a loss of sensory neuron populations or a loss of specific types of neurons (Airaksinen and Saarma, 2002; Ernsberger, 2008). Moreover, GDNF/RET signaling plays crucial roles in renal development (Costantini and Shakya, 2006) and the regulation of spermatogonia differentiation (Meng et al., 2000). In addition, RET mutations have been found to cause several human diseases, such as papillary thyroid carcinoma, multiple endocrine neoplasia types 2A and 2B, and Hirschsprung’s disease. *Ret*-knockout mice exhibit a lack of enteric neurons and superior cervical ganglia, as well as renal agenesis or dysgenesis (Schuchardt et al., 1994;

Abbreviations: ARTN, artemin; BDNF, brain-derived neurotrophic factor; CNTF, ciliary neurotrophic factor; ERG, electroretinography; GDNF, glial-cell-line-derived neurotrophic factor; GFLs, GDNF-family ligands; INL, inner nuclear layer; IPL, inner plexiform layer; NGF, nerve growth factor; NRTN, neurturin; ONL, outer nuclear layer; OPL, outer plexiform layer; PSPN, persephin; RT, room temperature; TGF- β , transforming growth factor β ; WT, wild-type.

Moore et al., 1996). Furthermore, a previous study demonstrated that abnormal retinal activity in NRTN- or *Ret*-deficient mice was associated with abnormal process extension of horizontal cells and bipolar cells into the outer nuclear layer (ONL), as well as a severely disrupted OPL with very sparse dendrites and axons of horizontal cells (Brantley et al., 2008). These results suggest that RET signaling is involved in retinal development. However, *Ret*-deficient mice die before postnatal day 21; thus, further evaluation of their retinal phenotype in adulthood is lacking in the literature (Schuchardt et al., 1994).

The Cre-loxP system is widely used as a powerful genetic tool for generating conditional knockout mice. Researchers can use this system to investigate genes of interest in a tissue/cell- (spatial control) and/or time- (temporal control) specific manner when straight knockout of the genes of interest causes embryonic lethality. In this study, we aimed to investigate the function of *Ret* in the retina by generating conditional knockout mice using the Cre-loxP system. Although conditional *Ret*^{RET^{flloxEGFP}/RET^{flloxEGFP};Six3 Cre knockout mice have been reported, the long-term effect of this intervention on the retina remains unknown (Brantley et al., 2008). To overcome this limitation, we deleted *Ret* exclusively in the retina by crossing homozygous *Ret* conditional knockout mice (i.e., *Ret*^{lx/lx} mice) with mice expressing Cre recombinase under the control of the *Chx10* gene. The *Chx10* gene is specifically expressed in the retinal progenitor cells at the early stage of eye development (E11.5), followed by a restricted expression in the bipolar cells as the progenitor cells differentiate and exit the cell cycle (Rowan and Cepko, 2004). We analyzed the retinal network in mature and aged *Chx10-Cre;C-Ret*^{lx/lx} mice and investigated the alteration in the ultrastructure of synaptic ribbons in *Chx10-Cre;C-Ret*^{lx/lx} mice specifically.}

MATERIALS AND METHODS

Animals

All animal procedures were performed according to the guidelines of the Association for Research in Vision and Ophthalmology Statement for the Use of Animals in Ophthalmic and Vision Research and were approved by the Institutional Animal Care and Use Committee of the National Taiwan University. *Ret*^{Ret < tm1.1Kln >} mice were generated by Dr. Klein (Kramer et al., 2007) by targeting a construct encompassing exons 11–13 of the *Ret* gene with Lox P sites flanking exon 12 (Figure 1A) (termed *C-Ret*^{lx/lx} mice hereafter). The generation of conditional knockout mice with *Ret* gene deletion in the retina was achieved by crossing *C-Ret*^{lx/lx} mice carrying LoxP sites flanking exon 12 of the *Ret* gene (Kramer et al., 2006) with mice expressing *Chx10-Cre* specifically in the retina (JAX: Stock No. 005105). All mice were housed in groups of four to five animals per cage in a room that was kept at 23 ± 1°C and 55% ± 5% humidity with a 12-h light/dark cycle, and were given *ad libitum* access to food and water. All mice used in our experiments were genotyped to confirm the absence of the *rd8* and *rd1* mutations as they may be present in vendor lines

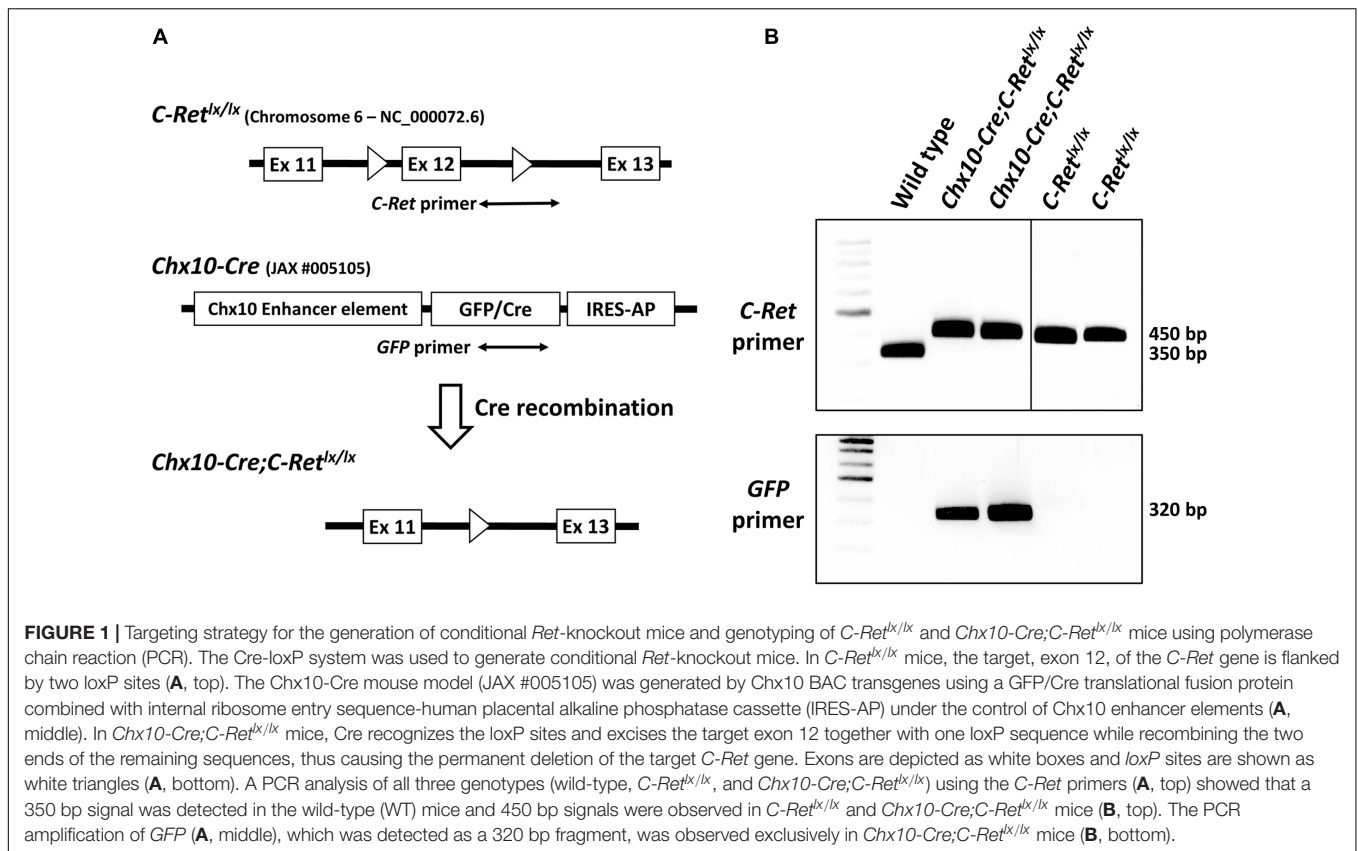
and subsequently confound ocular-induced mutant phenotypes (Errijgers et al., 2007; Mattapallil et al., 2012).

Mouse Genotyping

Mice were genotyped and verified using polymerase chain reaction (PCR) analysis. For genotyping, genomic DNA was isolated from a section of mouse tail, optic nerve and retina using an Aquadient™ kit (Bio-Rad, Richmond, CA, United States) according to the manufacturer's instructions. Mice homozygous for *C-Ret*^{lx/lx} were identified using the *C-Ret* forward (5'-CCA ACA GTA GCC TCT GTG TAA CCC C-3') and reverse (5'-GCA GTC TCT CCA TGG ACA TGG TAG CC-3') primers span the loxP in intron 12 (Figure 1A, top). Optic atrophy type 1 (*Opa1*) forward (5'-GAG CTG AGA GGG AGT GAA GAG AGG-3') and reverse (5'-CCC AAA ACT CCT TTA TCC CAG TGA C-3') primers could serve as the positive control. Furthermore, the *Chx10-Cre* mice carried *EGFP* fused with Cre recombinase; therefore, primers that amplify *EGFP* were also used to detect the presence of Cre recombinase. The thermal cycling conditions consisted of 30 cycles of 30 s at 94°C, 30 s at 55°C, and 50 s at 72°C. Reactions contained 200 ng of template DNA, 0.5 μM primers, 100 μM dNTPs, 9% glycerol, 2.5 U of *Taq* polymerase, 1.8 mM MgCl₂, and 1× PCR buffer (GIBCO BRL) in a volume of 20 μL. The PCR products were resolved via 2% agarose gel electrophoresis using Gel Red (Invitrogen/Life Technologies) as the visualizing dye. The DNA bands were visualized using a ChemiDoc Imaging System (Bio-Rad).

Electroretinography

Electroretinography was performed as described previously (Wang et al., 2010). After 12 h of adaptation in the dark, the mice were prepared for the ERG recordings using an Espion ERG System (Diagnosys LLC; Lowell, MA, United States) under dim red light. The animals were kept on a heating pad (Mycoal, Tochigi, Japan) during the ERG recordings, to maintain a constant body temperature. Mice were anesthetized via intraperitoneal injection of 0.1 mL of a mixed solution (1 mL of ketamine at 100 mg/mL and 0.1 mL of xylazine at 20 mg/mL in 8.9 mL of PBS) per 10 g of body weight, and pupils were dilated with topical 2.5% phenylephrine hydrochloride and 1% tropicamide. The test protocol consisted of 11 dark-adapted and nine light-adapted steps. The light intensities of the stimuli used for scotopic serial intensity ERG were -3.6, -3.2, -2.8, -2.4, -2.0, -1.6, -1.2, -0.6, 0.0, 0.4, and 0.9 log cd.s/m² in sequence. The intervals between each stimulus varied from 2 to 30 s, and the number of repeats varied from 10 to 4 times. After the completion of dark-adapted recordings, the animals were exposed to a full-field 30 cd/m² white background for 10 min; subsequent steps were delivered on top of this continuous background. The single-flash stimuli applied after light adaptation consisted of -0.1, 0.1, 0.3, 0.8, 1.0, 1.2, and 1.47 log cd.s/m². The intervals between each stimulus varied from 1 to 10 s, and the number of repeats varied from 3 to 10 times. A digital band-pass filter ranging from 0.3 to 300 Hz was used to isolate signals after the waves were recorded. The a-wave amplitude was measured from the baseline to the trough of the a-wave, and the b-wave



was measured from the trough of the a-wave to the peak of the b-wave.

Tissue Preparation

Mice were sacrificed at 2, 4, 12, and 24 months of age and their eyes were enucleated and fixed in 4% paraformaldehyde (PFA) in PBS for 1 h at room temperature (RT). For a better retinal infiltration of 4% PFA, corneas were partially removed and then placed in 4% PFA at 4°C for ~1 h. After washing in PBS three times, the tissues were incubated in a 30% sucrose solution in PBS at 4°C for 3 days. Tissues were embedded in optimum cutting temperature (OCT) compound (Thermo, Pittsburgh, PA, United States), snap frozen in liquid nitrogen, and immediately stored at -80°C. Cryosections (14 μm in thickness) were cut and collected on slides (Matsunami, Osaka, Japan). All slides were stored at -80°C before use. Before any staining process, the slides were air dried for 15 min and washed in PBS.

Hematoxylin Staining

Sections were stained with hematoxylin for 1 min, then washed with running water for 5 min. The stained sections were mounted with an aqueous mounting medium (EMS, Hatfield, PA, United States) and viewed under a microscope (Olympus CH-2 system, Tokyo, Japan). The brightness and contrast of photomicrographs were adjusted for maximum clarity using Adobe Photoshop CS5 (Adobe Systems, San Jose, CA,

United States). The retinas of three mice in each group underwent further histological analysis.

Immunohistochemistry

Sections were blocked with blocking buffer [5% fetal bovine serum (FBS) in PBS containing 0.1% Triton X-100] for 1 h at RT, followed by incubation with the primary antibodies (Table 1) diluted in 3% FBS in PBS at 4°C overnight. The sections were subsequently incubated with the secondary antibodies for 1 h at RT. After washing three times in PBS, they were mounted with mounting medium (EMS, Hatfield, PA, United States) and viewed under a Leica DM6000 Confocal Fluorescence Imaging Microscope (Leica Microsystems, Wetzlar, Germany).

Transmission Electron Microscopy and Quantification

Retinas were isolated and fixed in 2% glutaraldehyde and 2% PFA in 0.1 M PB at 4°C overnight. After postfixing in 1% osmium tetroxide for 1 h, tissue samples were dehydrated in a graded ethanol series and embedded in epoxy resin (EMS, Hatfield, PA, United States). Ultrathin sections (70 nm in thickness) were collected on copper grids and stained with uranyl acetate and lead citrate before examination under a Hitachi H-7100 electron microscope (Hitachi, Tokyo, Japan) equipped with a Gatan 832 digital camera (Gatan, Inc., Pleasanton, CA, United States).

For the quantification of synaptic ribbon conditions, images of the OPL were taken at a magnification of 40,000X. Approximately

TABLE 1 | List of antibodies applied for immunohistochemistry.

| Antigen | Antiserum | Cell type | Source | Catalog | Dilution factor |
|-----------------------|--|-----------------------------------|--------------------------|---------------|-----------------|
| α -interneixin | Mouse anti-interneixin, α , C-terminus, clone 2E3 | Horizontal cell and ganglion cell | Millipore | MAB5224 | 1:100 |
| PKC- α | Mouse anti-PKC- α (H-7) | Rod bipolar cell | Santa Cruz Biotechnology | Sc-8393 | 1:100 |
| PKC- α | Rabbit anti-PKC- α (H-300) | Rod bipolar cell | Santa Cruz Biotechnology | Sc-10800 | 1:100 |
| Synaptophysin | Rabbit anti-synaptophysin | Photoreceptor | Abcam | Ab-14692 | 1:100 |
| Calbindin | Rabbit anti-calbindin | Horizontal cell | Invitrogen | PA1-931 | 1:500 |
| PSD-95 | Mouse anti-PSD95 | Photoreceptor | NeuroMab | 75-028 | 1:500 |
| EGFP | Rabbit anti-(GFP) | GFP expressing cells | Millipore | Ab-3080 | 1:500 |
| Mouse IgG | Goat anti-mouse IgG Alexa 488 and 594 | | Invitrogen | A11001 A11005 | 1:200 |
| Rabbit IgG | Goat anti-rabbit IgG Alexa 488 and 594 | | Invitrogen | A11008 A11012 | 1:200 |

500 photoreceptor terminals for each age were examined and classified into different categories of rod-shaped ribbon profiles.

Histological Quantification

The thickness of the ONL and inner nuclear layer (INL) was quantified from single optical sections. Images were taken at a distance of 200 μm from the optic disc and within fields with a size of 300 \times 800 μm^2 , which was modified from previous studies that chose the area of approximately 200–500 μm away from the optic nerve for quantification (Berger et al., 2014; Mead et al., 2014). Five images per retina were analyzed in three mice per group.

Statistical Analysis

All experimental data were assessed by an operator blinded to the genetic condition. The results were presented as the mean \pm standard error of the mean (SEM) and statistical significance was determined by independent Student's *t*-test. $P < 0.05$ was considered significant. All analyses were performed using SPSS (IBM SPSS Statistics for Windows, Version 21.0, IBM Corp. Armonk, NY, United States) and GraphPad Prism 5.0a (GraphPad Software Inc., San Diego, CA, United States).

RESULTS

Generation of Conditional Knockout Mice

To detect the *C-Ret*^{lx/lx} allele in both *Chx10-Cre;C-Ret*^{lx/lx} and *C-Ret*^{lx/lx} mice, total DNA from wild-type (WT) and transgenic mice was subjected to PCR analysis with *C-Ret* primers spanning the intron 12 loxP sequence (Figure 1A, top). In WT mice (without the loxP insertion), the 350 bp amplicon was detected using the *C-Ret* primers. In contrast, given that *C-Ret*^{lx/lx} and *Chx10-Cre;C-Ret*^{lx/lx} mice contained loxP sequences, they yielded an amplicon of 450 bp instead (Figure 1B, top). Because the *Chx10-Cre* mouse model (JAX: Stock No. 005105) was generated by *Chx10* BAC transgenes using a “GFP/Cre translational fusion protein” (Figure 1A, middle), we used GFP primers to determine the presence of Cre. Consequently, we found that a 320 bp

fragment was detected exclusively in *Chx10-Cre;C-Ret*^{lx/lx} mice, and not in WT or *C-Ret*^{lx/lx} mice (Figure 1B, bottom).

Conditional Knockout *C-Ret* in Retina and Expression of *Chx10-Cre*

To validate whether exon 12 of the *C-Ret* gene was deleted in the retina of *Chx10-Cre;C-Ret*^{lx/lx} mice, we performed PCR analysis using *C-Ret* primers on DNA extracted from retina and optic nerve of *C-Ret*^{lx/lx} and *Chx10-Cre;C-Ret*^{lx/lx} mice. We found that PCR could amplify *C-Ret* in *C-Ret*^{lx/lx} retina, but barely in *Chx10-Cre;C-Ret*^{lx/lx} retina, indicating that exon 12 of the *C-Ret* gene was deleted in most of the retina cells of *Chx10-Cre;C-Ret*^{lx/lx} mice (Figure 2A, top). On the other hand, PCR could amplify *C-Ret* from optic nerves in both *C-Ret*^{lx/lx} and *Chx10-Cre;C-Ret*^{lx/lx} mice. In addition, PCR amplification with *Opa1* primers was used to make sure the DNA was successfully extracted from different regions of eyeball and equally loading DNA amount for each lane (Figure 2A, bottom). To further validate the expression of Cre expression in *Chx10-Cre* mice, we did immunohistochemistry to label rod bipolar cells and GFP expressing cells using anti-PKC- α and anti-EGFP antibodies. Because the Cre protein on its own has the capacity to cross the membrane and translocate to the nucleus (Will et al., 2002), the IHC results showed GFP expression only in the nuclei of *Chx10-Cre;C-Ret*^{lx/lx} bipolar cells, while PKC- α expression was identified in the cytoplasm of bipolar cells in both *C-Ret*^{lx/lx} and *Chx10-Cre;C-Ret*^{lx/lx} mice (Figure 2B). Based on PCR and IHC analysis, *Chx10-Cre;C-Ret*^{lx/lx} mice were conditionally deleted the exon 12 of *C-Ret* gene in the retina.

In vivo Analyses of Retinal Function and Morphology in *Chx10-Cre;C-Ret*^{lx/lx} Mice

To determine the effect of *Ret* deficiency on retinal function, ERG was performed in 12-month-old *Chx10-Cre;C-Ret*^{lx/lx} and *C-Ret*^{lx/lx} mice (Figure 3). The *C-Ret*^{lx/lx} mice showed a normal ERG pattern of series intensity stimulation. As the flash intensity of the scotopic phase increased, the amplitude of the a-wave and b-wave increased. The a-wave represents the activity of the photoreceptors, whereas the b-wave reflects bipolar cell activity. The scotopic ERG of *Chx10-Cre;C-Ret*^{lx/lx} mice revealed a selective reduction of b-waves, with relative preservation of

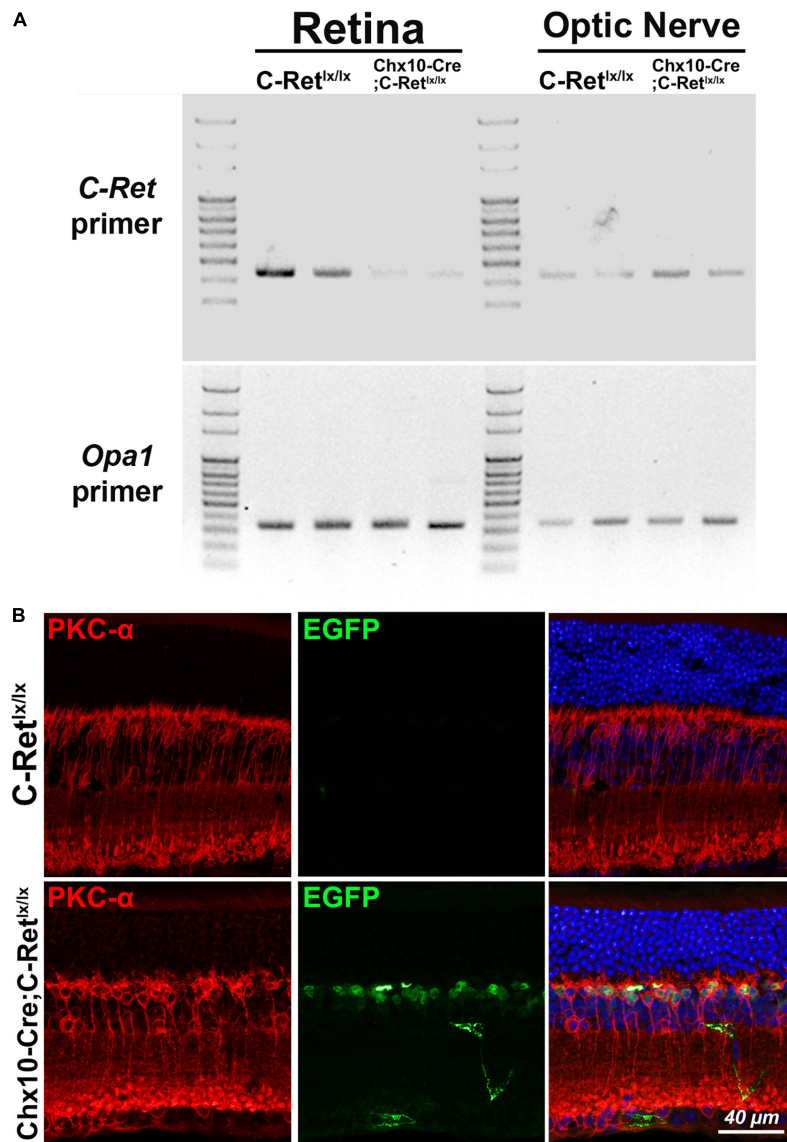
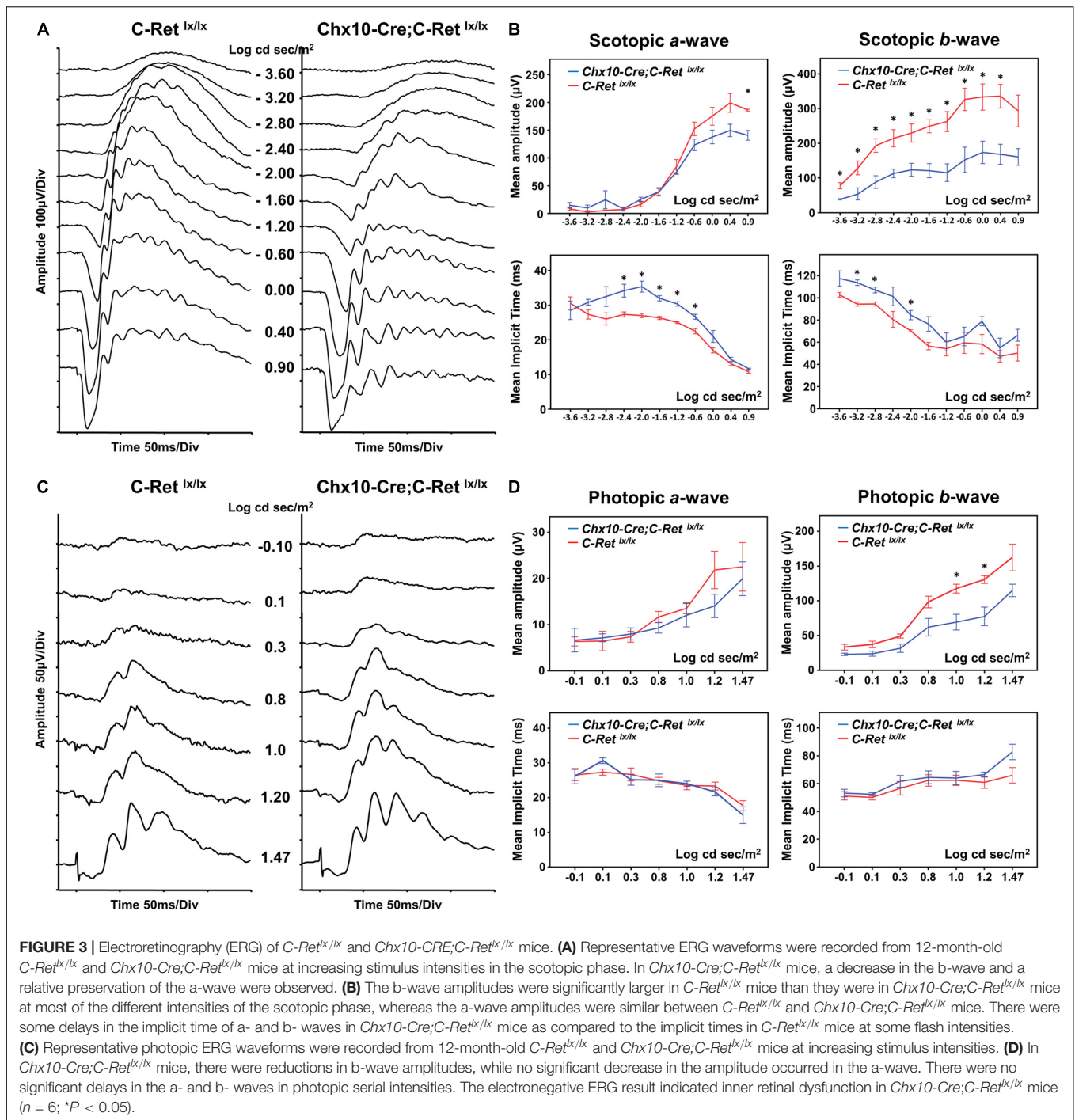


FIGURE 2 | Amplification of *C-Ret* gene and immunohistochemistry of GFP in *C-Ret*^{lx/lx} and *Chx10-Cre;C-Ret*^{lx/lx} mice. **(A, top)** Polymerase chain reaction (PCR) was performed using *C-Ret* primers to screen the presence of exon 12 within the *C-Ret* gene. The results showed that barely any amplification occurred in the retinae of *Chx10-Cre;C-Ret*^{lx/lx} mice compared to that in the retinae of *C-Ret*^{lx/lx} mice. PCR was able to amplify *C-Ret* gene from optic nerve in both *C-Ret*^{lx/lx} and *Chx10-Cre;C-Ret*^{lx/lx} mice. **(A, bottom)** PCR analysis using *Opa1* primers showed equally amplification between *C-Ret*^{lx/lx} and *Chx10-Cre;C-Ret*^{lx/lx} mice in retinae and optic nerve tissue. **(B)** Retinal sections of animals aged 12 months were immunostained with anti-PKC-α (red) and anti-EGFP (green) antibodies to label rod bipolar and GFP expressing cells, respectively, followed by counterstaining with Hoechst dye, to indicate cell nuclei (blue). PKC-α (red) was expressed in cytoplasm of bipolar cells in *C-Ret*^{lx/lx} and *Chx10-Cre;C-Ret*^{lx/lx} mice; however, the GFP was only expressed in the nucleus of bipolar cells of *Chx10-Cre;C-Ret*^{lx/lx} mice due to fusion with Cre protein, which has the capacity to cross the membrane and translocate to the nucleus.

a-waves in the scotopic phase (**Figures 3A,B**). The implicit times of a- and b- waves were more delayed in *Chx10-Cre;C-Ret*^{lx/lx} mice (**Figure 3B**) ($n = 6$; $*P < 0.05$). In photopic serial intensity ERG, there were reductions in amplitude of a- and b- waves in *Chx10-Cre;C-Ret*^{lx/lx} mice, which were statistically significant in some intensities of b-waves. However, there was no obvious difference in the implicit time of a- and b- waves in photopic responses between *Chx10-Cre;C-Ret*^{lx/lx} and *C-Ret*^{lx/lx} mice. The ERG recordings suggested that the *Chx10-Cre;C-Ret*^{lx/lx}

mice may exhibit a greater effect on the function of bipolar cells. Furthermore, these tracings were similar to those of an electronegative ERG corresponding to inner retinal dysfunction.

Hematoxylin staining was used to examine whether the *Chx10-Cre;C-Ret*^{lx/lx} mice had morphological alterations in the retina (**Figure 4**). We observed that, compared with *C-Ret*^{lx/lx} mice (**Figures 4A–D**), the retinae of *Chx10-Cre;C-Ret*^{lx/lx} mice seemed to exhibit a progressive decrease in the thickness of the ONL, OPL, INL, and inner plexiform layer (IPL) (**Figures 4E–H**).

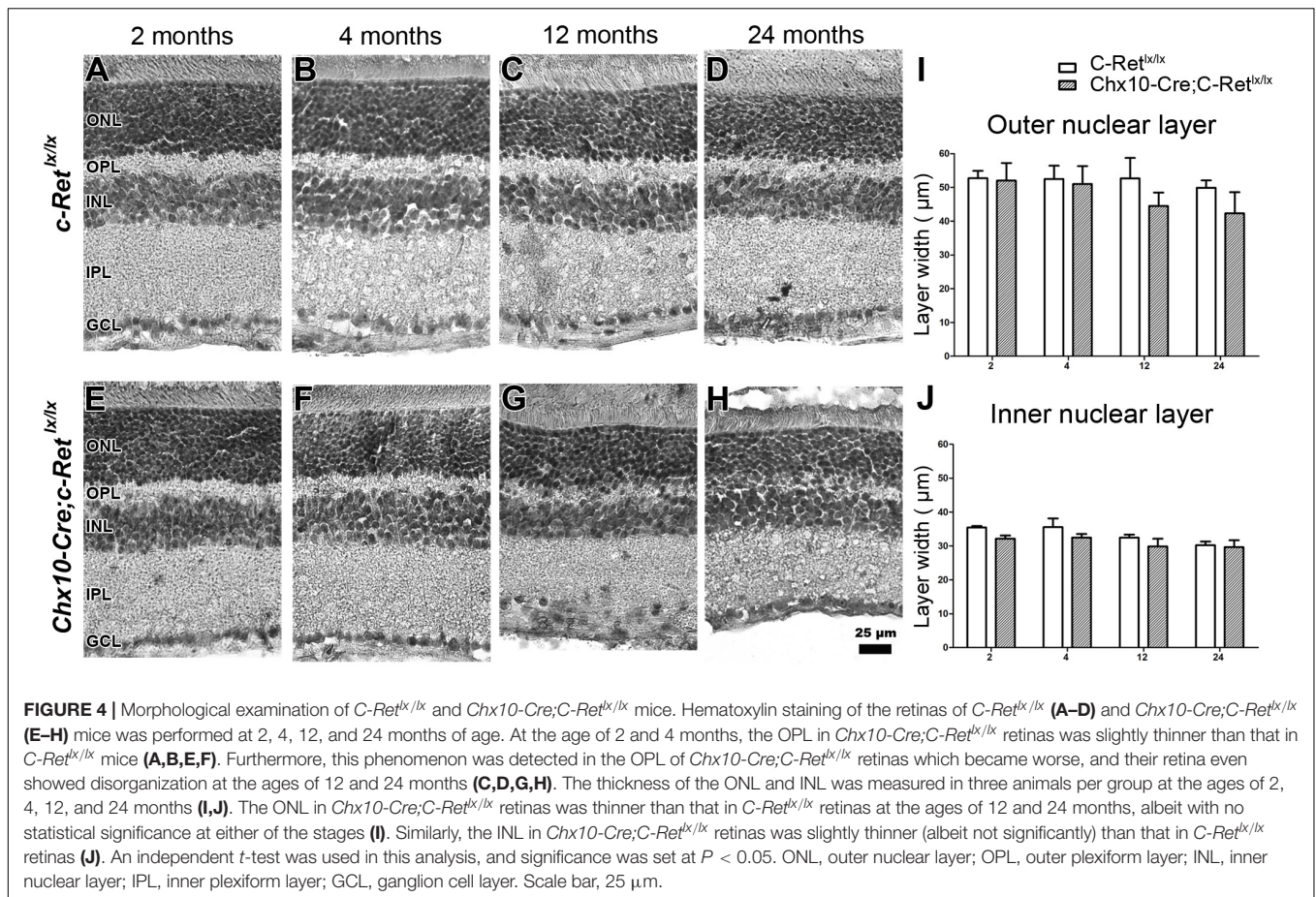


Some nuclei in the ONL invaded the OPL in *Chx10-Cre;C-Ret^{lx/lx}* mice at 12 months of age, which became more obvious in these animals at the age of 24 months. We then quantified the thickness of the ONL (Figure 4I) and INL (Figure 4J) using morphometric measurements. Although there was no statistically significant difference in the thickness of the ONL and INL between the *Chx10-Cre;C-Ret^{lx/lx}* and *C-Ret^{lx/lx}* retinas, we found that the thickness of the ONL in *Chx10-Cre;C-Ret^{lx/lx}* mice showed a 15.4% reduction at 12 months and a 16.3% reduction at

24 months. This observation suggests that the retinal morphology in *Chx10-Cre;C-Ret^{lx/lx}* mice is altered at older ages.

Immunohistochemistry of Horizontal Cells and Rod Bipolar Cells in *Chx10-Cre;C-Ret^{lx/lx}* Mice

To identify the components that are potentially altered in the OPL, IHC was performed to label the horizontal cells and



rod bipolar cells in mouse retinas. Bipolar cells and horizontal cells are the second-order neurons that form synapses with photoreceptor terminals in the OPL. A previous study indicated that α -internexin is expressed in horizontal cells and may be used as a marker of these cells in the study of the mouse retina (Chien and Liem, 1995). Therefore, an anti- α -internexin antibody was used to detect the processes of horizontal cells (Figures 5A–H). In *C-Ret^{lox/lox}* mice, horizontal cells possessed arborizing processes in the OPL of mice aged 2–24 months (Figures 5A–D). In contrast, the processes of horizontal cells in *Chx10-Cre;C-Ret^{lox/lox}* mice were reduced at the ages of 2 and 4 months (Figures 5E,F), followed by a dramatic decrease at the ages of 12 and 24 months (Figures 5G,H). In order to obtain a second confirmation of changes in horizontal cells, the anti-calbindin antibody was applied to the sections, revealing a similar immunoreactivity pattern to that of α -internexin (Supplementary Figure 1). These results demonstrated that horizontal cells were affected in the conditional *Ret*-knockout mice.

The retinal rod bipolar cells expressed protein kinase C alpha (PKC- α), the distribution of which, within cells, is reportedly activity-dependent in the rat model (Gabriel et al., 2001). Thus, vertical sections of retinas were immunostained for PKC- α (Figures 5I–P). The immunoreactivity of PKC- α in *C-Ret^{lox/lox}* mice showed that the bipolar cells had their cell bodies and the cytosolic compartments in the INL, the dendritic processes in

the OPL, and the axon terminals in the innermost sublamina of the IPL (Figures 5I–L). A subpopulation of bipolar cells with axons terminating close to the ganglion cell layer was also observed. In *Chx10-Cre;C-Ret^{lox/lox}* mice, bipolar cells exhibited a normal organization pattern, as in *C-Ret^{lox/lox}* mice, and had well-preserved processes at the ages of 2 and 4 months (Figures 5M,N). However, at the ages of 12 and 24 months, some bipolar cells exhibited abnormal processes that sprouted into the ONL (Figures 5O,P). Furthermore, the aberrant processes tended to become longer and more numerous in aged *Chx10-Cre;C-Ret^{lox/lox}* mice. According to these observations, bipolar cells may also be altered in conditional *Ret*-knockout mice.

Alteration of Pre- and Post-synaptic Structures in *Chx10-Cre;C-Ret^{lox/lox}* Retinas

To determine whether the dendritic extensions of the rod bipolar cells change in synapses with photoreceptors, double IHC was performed. Given that synaptophysin is an integral membrane protein of synaptic vesicles, it is used to label synaptic structures in the terminals of photoreceptors (Nag and Wadhwa, 2001). Double immunohistochemistry using anti-PKC- α and anti-synaptophysin antibodies demonstrated that PKC- α -positive processes lay among synaptophysin-positive terminals in

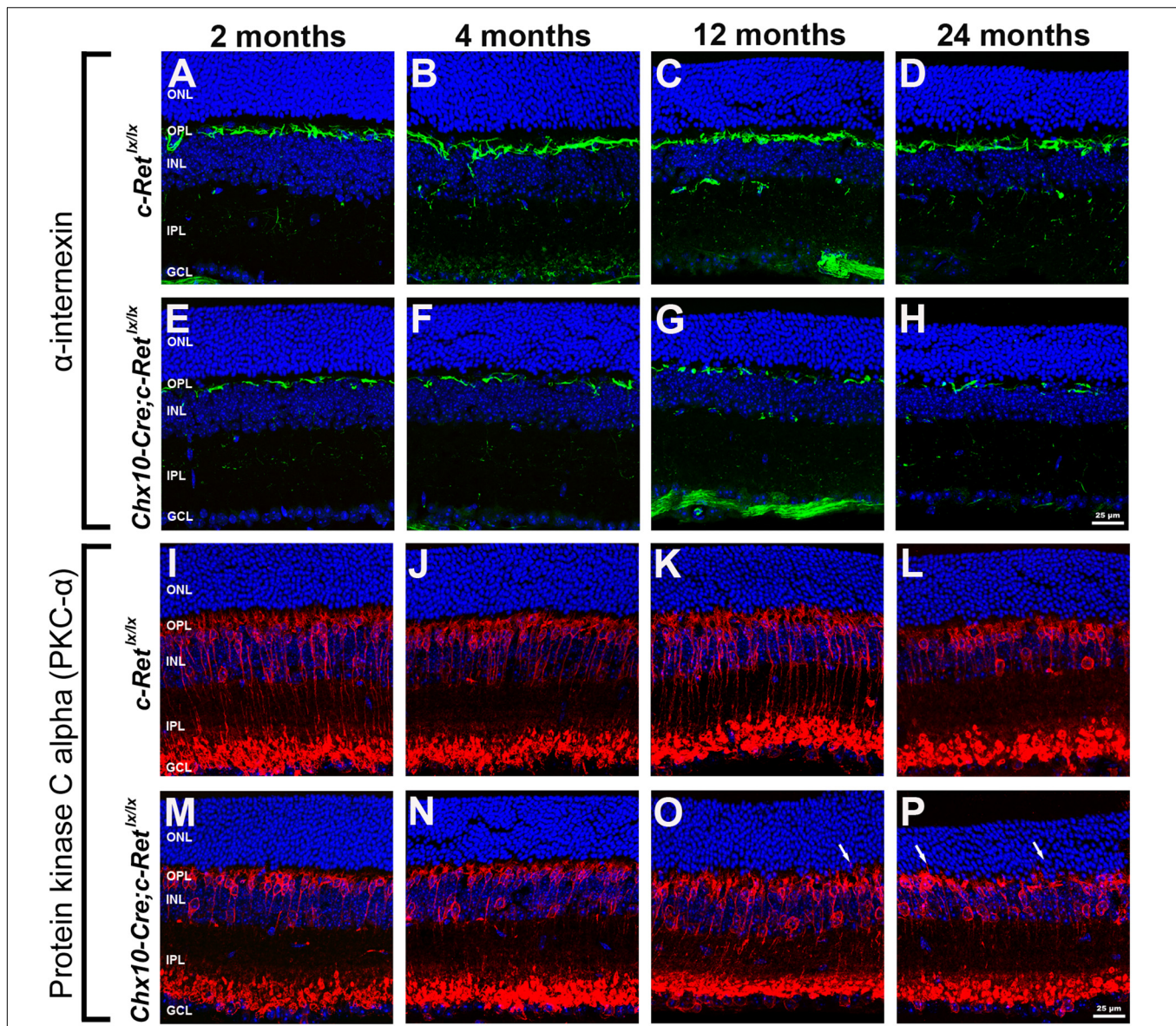


FIGURE 5 | Immunohistochemistry of horizontal cells and rod bipolar cells in *C-Ret^{lox/lox}* and *Chx10-Cre;C-Ret^{lox/lox}* retinas. Retinal sections of mice aged 2, 4, 12, and 24 months were immunostained with an anti- α -interneuron antibody (green, **A–H**) or an anti-PKC- α antibody (green, **I–P**), to label horizontal cells and rod bipolar cells, respectively, followed by counterstaining with Hoechst dye, to reveal cell nuclei (blue). Compared with *C-Ret^{lox/lox}* mice (**A–D**), the processes of horizontal cells were sparse and discontinuous in *Chx10-Cre;C-Ret^{lox/lox}* mice and were even more deteriorated at the ages of 12 and 24 months (**E–H**). The processes of rod bipolar cells were similar between *C-Ret^{lox/lox}* (**I–L**) and *Chx10-Cre;C-Ret^{lox/lox}* (**M–P**) mice aged 2, 4, 12, and 24 months. However, some processes of rod bipolar cells extended into the ONL at the ages of 12 and 24 months in *Chx10-Cre;C-Ret^{lox/lox}* mice (**O,P**, arrows), which was not observed in *C-Ret^{lox/lox}* mice. ONL, outer nuclear layer; OPL, outer plexiform layer; INL, inner nuclear layer; IPL, inner plexiform layer; GCL, ganglion cell layer. Scale bar, 25 μ m.

the OPL of *C-Ret^{lox/lox}* mice (**Figures 6A–D**). A similar pattern was observed in *Chx10-Cre;C-Ret^{lox/lox}* mice aged 2 and 4 months that processes, i.e., most of the rod bipolar cells labeled by the anti-PKC- α antibody were associated with synaptophysin-labeled rod axon terminals in the OPL (**Figures 6E,F**). However, in *Chx10-Cre;C-Ret^{lox/lox}* mice aged 12 and 24 months, some PKC- α - and synaptophysin-positive processes were mislocalized in the ONL and synaptophysin-positive processes were also decreased (**Figures 6G,H**). In addition, the post-synaptic density protein 95

(PSD-95) was detected in the OPL (**Supplementary Figure 2**). A significant decrease of PSD-95 expression was found in *Chx10-Cre;C-Ret^{lox/lox}* mice aged 12 and 24 months, compared to *C-Ret^{lox/lox}* mice. The IHC results indicated that the synapses between rod bipolar cells and photoreceptors were affected in conditional *Ret*-knockout mice.

To further confirm the morphological changes observed in the OPL of *Chx10-Cre;C-Ret^{lox/lox}* mice, we performed TEM observations and identified ribbon synapses at the outer retina

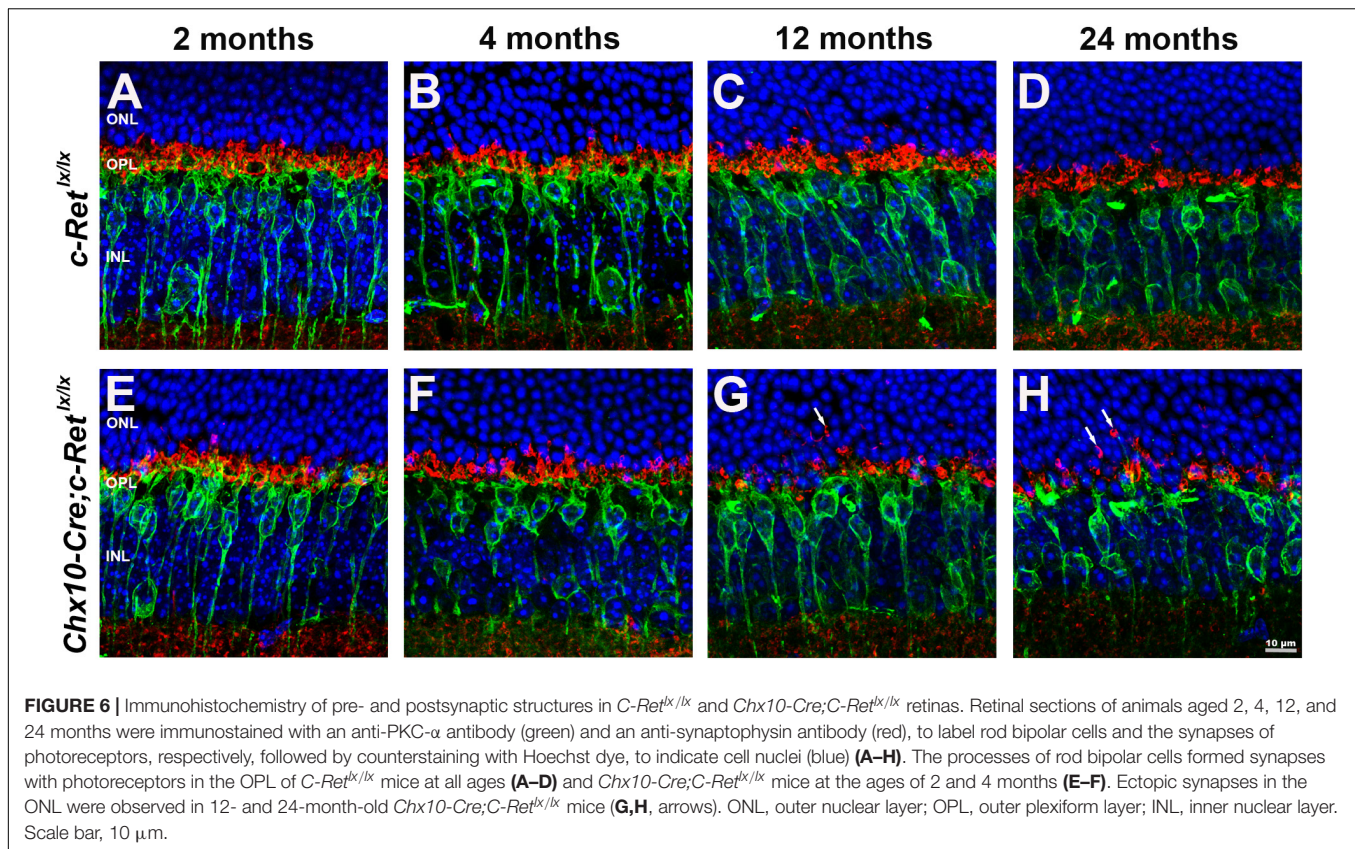
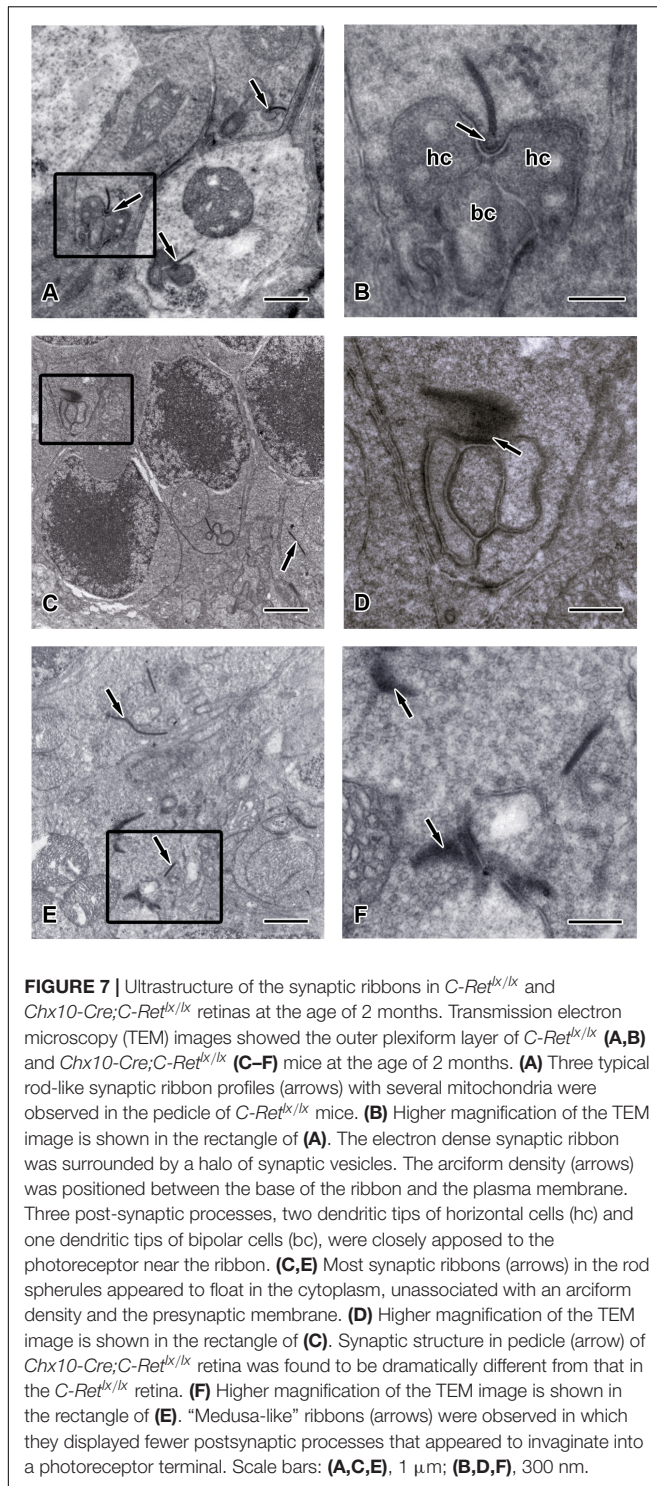


FIGURE 6 | Immunohistochemistry of pre- and postsynaptic structures in *C-Ret^{lx/lx}* and *Chx10-Cre;C-Ret^{lx/lx}* retinas. Retinal sections of animals aged 2, 4, 12, and 24 months were immunostained with an anti-PKC- α antibody (green) and an anti-synaptophysin antibody (red), to label rod bipolar cells and the synapses of photoreceptors, respectively, followed by counterstaining with Hoechst dye, to indicate cell nuclei (blue) (A–H). The processes of rod bipolar cells formed synapses with photoreceptors in the OPL of *C-Ret^{lx/lx}* mice at all ages (A–D) and *Chx10-Cre;C-Ret^{lx/lx}* mice at the ages of 2 and 4 months (E–F). Ectopic synapses in the ONL were observed in 12- and 24-month-old *Chx10-Cre;C-Ret^{lx/lx}* mice (G,H, arrows). ONL, outer nuclear layer; OPL, outer plexiform layer; INL, inner nuclear layer. Scale bar, 10 μ m.

of *C-Ret^{lx/lx}* and *Chx10-Cre;C-Ret^{lx/lx}* mice aged 2 months (Figure 7) and 12 months (Figure 8). The photoreceptor ribbon synapses of *C-Ret^{lx/lx}* mice exhibited a varying number of rod-shaped profiles in photoreceptor terminals (Figures 7A,B). Ribbon ultrastructure was defined by the central presynaptic ribbon opposed by two postsynaptic horizontal cell processes. The synaptic ribbon displayed its typical plate-like shape, extending perpendicular to the presynaptic membrane into the cytoplasm. Although, plentiful synaptic ribbons in *Chx10-Cre;C-Ret^{lx/lx}* mice aged 2 months, having roughly the same length and appearance as those in *C-Ret^{lx/lx}* terminals, were observed, they were usually found to be “floating” in the cytoplasm instead of anchored to other synaptic structures (Figures 7C–E). Besides, the number of “Medusa-like” ribbons seemed to be increased and the synaptic ribbons were observed reduced in height and swollen shaped (Figures 7E,F). Therefore, the synaptic ribbon is surrounded by a halo of synaptic vesicles, as they do in the *C-Ret^{lx/lx}* retina.

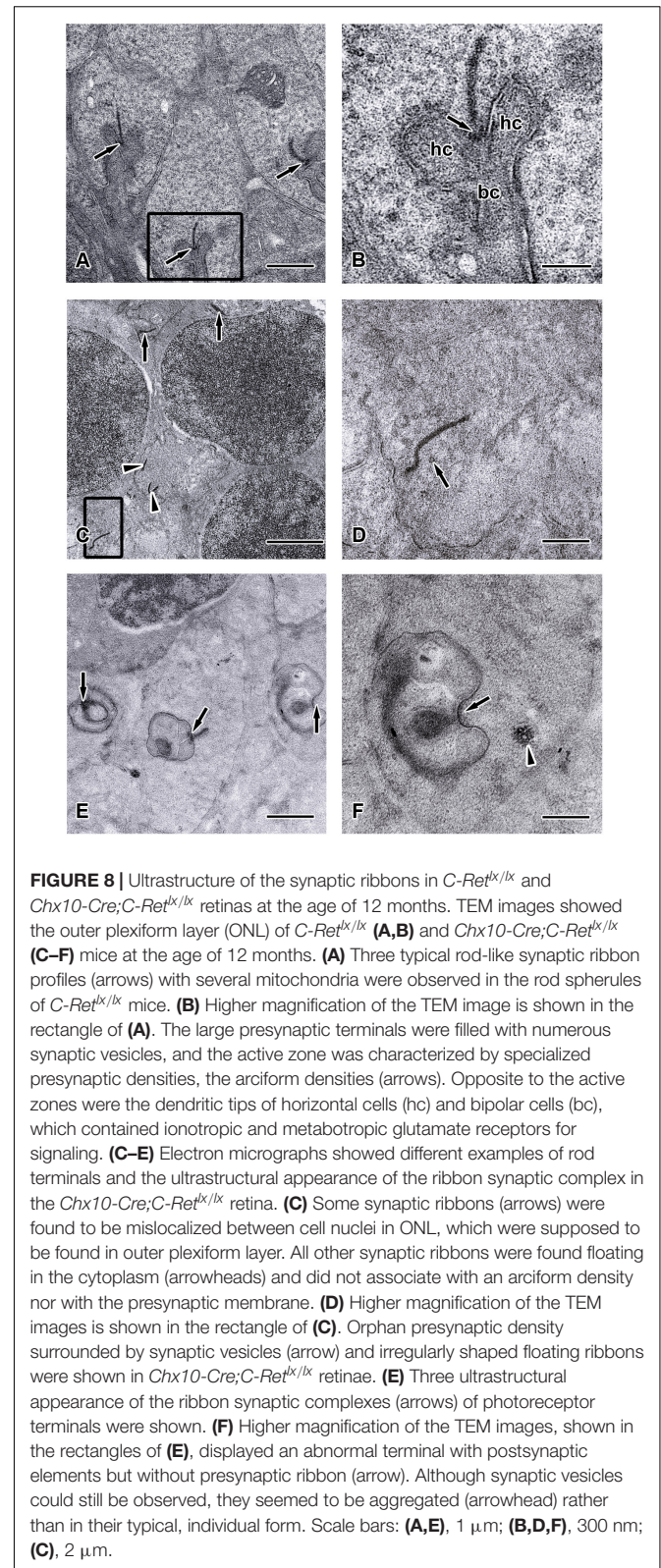
Furthermore, the appearance of the ribbon synaptic complexes in the 12-month *Chx10-Cre;C-Ret^{lx/lx}* mice retinae differed significantly from those in the *C-Ret^{lx/lx}* retinae. Normally, a rod synaptic terminal in *C-Ret^{lx/lx}* retina contained a single ribbon synaptic site (Figure 8A), where glutamate was released onto the postsynaptic elements, horizontal cell processes and rod bipolar cell dendrites. The postsynaptic elements invaginated into the rod terminal and formed a triadic or tetradic configuration adjacent to the ribbon site

(Figure 8B). However, most of the ribbons in the retinae of 12-month-old *Chx10-Cre;C-Ret^{lx/lx}* mice were not docked at the synaptic site (i.e., they floated freely in the cytoplasm) (Figures 8C,D). Many empty rod terminals without presynaptic ribbons and postsynaptic invaginating elements were found in *Chx10-Cre;C-Ret^{lx/lx}* mice (Figure 8E). In addition, the number of synaptic vesicles was decreased near synapses (Figure 8D) and found in clumps rather than distributed evenly in the pedicle (Figure 8F). Following these observations, we classified the synaptic ribbons into two categories: rod-shaped and non-rod-shaped, based on their general morphological features; this was followed by quantification of the synaptic ribbons. Representative examples of the rod-shaped ribbons anchored at the active zone, where exocytosis of synaptic vesicles occurred, are shown in Figure 9A and the quantitative data are summarized in Figure 9B. 87.1 and 86.3% of rod photoreceptor ribbon profiles were presynaptically anchored and rod-shaped in *C-Ret^{lx/lx}* mice aged 2 and 12 months, respectively. In contrast, a significant decrease was found in the *Chx10-Cre;C-Ret^{lx/lx}* mice whereby only 62.4% of rod photoreceptor ribbon profiles were presynaptically anchored and rod-shaped at the age of 2 months; this proportion only worsened at the age of 12 months (54.2% of rod photoreceptor ribbons). The aforementioned TEM results suggest that the loss of *Ret* causes a structural defect in the synaptic connection between photoreceptors and bipolar cells. Ultimately, this finding may underlie the abnormal ERG b-wave observed in *Chx10-Cre;C-Ret^{lx/lx}* mice.



DISCUSSION

In this study, we generated retinal *Ret*-specific knockout mice using the Cre/loxP system and demonstrated a possible role for *Ret* in retinal function. First, we found severely abnormal ERG patterns, especially those of b-waves, in conditional *Ret*-knockout



retinas. Second, we identified gradually reduced levels of immunoreactivity for α -internexin—a marker of processes of horizontal cells—as *Chx10-Cre;C-Ret^{lox/lox}* mice increased in age.

Third, deficiency of *Ret* in the retina caused the mislocalization of synapses in the ONL, as demonstrated by immunostaining for PKC- α and synaptophysin. Finally, ultrastructural observations of conditional *Ret*-knockout retinas revealed that the synaptic ribbons were immature and not fully assembled, which may explain the abnormal ERG results.

The function of *Ret* in the retina was well assessed by full-field ERG in previous studies. *Ret* hypomorphic mice, which exhibit severely reduced *Ret* activity, do not survive beyond 3 weeks and display significantly reduced scotopic a-waves, b-waves, and photopic b-waves at postnatal day 18 (Brantley et al., 2008). In this study, the *Chx10-Cre;C-Ret^{lx/lx}* mice, which had conditional retinal *Ret* deficiency, exhibited a prolonged survival time and a selective reduction in b-waves, but normal a-waves, on ERG performed at 12 months of age. As such, this waveform was deemed an electronegative ERG and suggested a dysfunction of the ON bipolar cells. In addition to bipolar cells, it was also hypothesized that reduced b-waves could result from the impaired horizontal cells if their inhibition to bipolar cells was switched off (Goetze et al., 2010). Taken together, these results indicate that sufficient *Ret* expression is required for normal retinal function and development.

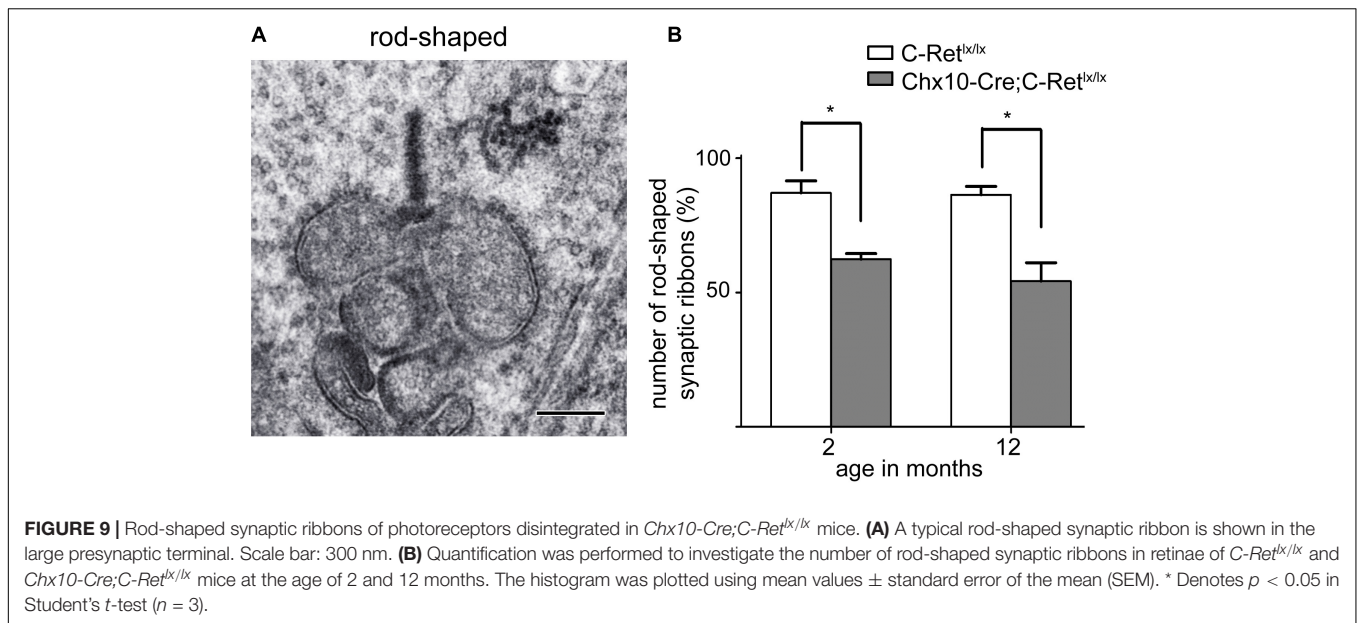
GDNF and other GFLs (ARTN, NRTN, and PSPN) share the RET receptor tyrosine kinase as their common signaling receptor. A previous study revealed a thinner and disorganized OPL in *NRTN^{-/-}* mice, suggesting that the aberrant morphology of photoreceptors, bipolar cells, and horizontal cells was caused by NRTN deficiency (Brantley et al., 2008). Moreover, GDNF can increase the proliferation, promote the differentiation, and prevent the programmed death of chicken rod photoreceptors, as assessed using re-aggregated retinal spheroids as an *in vitro* assay model (Rothermel and Layer, 2003). Another GDNF-family receptor alpha-4 (GFR α 4)-deficient retinal culture study showed a decrease in the number of amacrine cells, horizontal cells, and blue-sensitive cone photoreceptors in this system (Rothermel et al., 2006). In our study, the immunoreactivities of α -internexin and PKC- α were altered in *Chx10-Cre;C-Ret^{lx/lx}* mice. These results indicate that *Ret* dysfunction may trigger an abnormal morphology in horizontal cells and bipolar cell processes, and provided evidence that GFLs, GDNF-family receptors (GFRs), or the RET receptor tyrosine kinase can specifically affect distinct photoreceptors and other retinal cell subpopulations.

It was reported that GDNF can be produced by glial cells to increase the survival rate of a retinal ganglion or photoreceptor cells in different experimental models, such as the rescue of retinal ganglion cells after axotomy (Koeberle and Ball, 1998), the delivery of a protective effect in mice with glaucoma (Johnson et al., 2011), or the protection of photoreceptors in the *rd1* mouse (Frasson et al., 1999). Furthermore, GDNF also moderately protected the rat retina from ischemia-reperfusion injury, possibly by preventing apoptosis in retinal cells (Wu et al., 2004). These previous studies suggested that, in the absence of GDNF, retinal cells lose a protective factor, which might lead to serious retinal dysfunction or degeneration. In addition, a previous study demonstrated that GDNF partially restored ureteric branching morphogenesis in *Ret*-deficient mice with

severe renal hypodysplasia, possibly through the induction of Met phosphorylation, rather than through RET signaling (Popsueva et al., 2003). This implies that it is also possible that GDNF partially signals independently of RET through the GDNF-family receptor alpha-1 (GFR α 1) and Met phosphorylation in the retina. In fact, the GFL-GFR α 1 complex activates Met kinase indirectly via Src kinases in the absence of RET kinase (Popsueva et al., 2003). The GFLs can also interact directly with heparan sulfate proteoglycans to activate Met kinase, which might be mediated by a neural cell adhesion molecule (N-CAM) (Sariola and Saarma, 2003). Our results revealed that the thickness of the ONL was decreased at the stage of 12 and 24 months; however, there were no significant differences between *C-Ret^{lx/lx}* and *Chx10-Cre;C-Ret^{lx/lx}* mice. Moreover, the processes of horizontal cells were significantly reduced, and the immunoreactivities of synaptophysin and PKC- α demonstrated the presence of mislocalized synapses in the ONL. Despite these alterations, the retinas of *Chx10-Cre;C-Ret^{lx/lx}* mice did not show severe disorganization. We speculated that GDNF signaling independently of RET and via GFR α 1 might explain why the retinas of *Chx10-Cre;C-Ret^{lx/lx}* mice failed to show severe dysfunction or disorganization.

GDNF is also known as one of the neurotrophic factors that play key roles in the development and survival of neurons. Neurotrophic factors generally include the neurotrophin family [NGF, BDNF, neurotrophin-3 (NT-3), and NT-4/5], the GDNF family (GDNF, NRTN, ARTN, and PSPN), and the CNTF, which is a member of the interleukin 6 (IL-6) family of cytokines. Different factors can act in a sequential, simultaneous, additive (synergistical), or mutual-inhibition fashion. For instance, subpopulations of developing sensory and motor neurons are dependent on the simultaneous action of GDNF and BDNF (Henderson, 1996). Moreover, a combination of GDNF and CNTF was reported to afford higher protection to photoreceptors in a retinal degeneration (rd) mouse (Ogilvie et al., 2000). In our study, *Chx10-Cre;C-Ret^{lx/lx}* mouse retinas had deletion of RET, which is the canonical GDNF receptor, but did not show severe dysfunction or disorganization. According to the studies mentioned above, another explanation for the resulting mild dysfunction following RET deletion is that the remaining neurotrophic factors—which remained unaffected—compensated for the effects of knocking out the RET signaling pathway. However, this study did not investigate the neurotrophic factors or possible signaling pathways independent of RET that may play roles in the retinas of *Chx10-Cre;C-Ret^{lx/lx}* mice. Therefore, further research is required to clarify the mechanisms underlying these observations.

The ribbon complex of retinal photoreceptor synapses represents a specialization of the cytomatrix at the active zone that is present at conventional synapses. The active zones of synapses are highly organized structures designed for the regulated and site-specific release of neurotransmitters. The function of photoreceptor ribbons was suggested to be the continuous shuttling of vesicles to the active zone, for fusion and the release of glutamate (Lenzi and von Gersdorff, 2001). In a previous study, ribbons in *Bassoon* (*Bsn*)-mutant mouse retinas did not attach to the active zone, thus potentially



resulting in the failure of synaptic transmission. Moreover, the a-waves of the ERG recordings performed in the *Bsn*-mutant mouse were not affected, whereas their b-waves, representing the response of the ON bipolar cells, were significantly reduced in amplitude and prolonged in implicit time (Dick et al., 2003). Our ultrastructural observation revealed the inappropriate assembly of synaptic ribbons, which then failed to anchor themselves to the active zone. Moreover, a severely affected ERG was recorded in the retinas of *Chx10-Cre;C-Ret^{lox/lox}* mice, implying that conditional deletion of *Ret* in the retina may cause a dysfunction in synaptic transmission. In addition, other findings demonstrated that the co-administration of the fibroblast growth factor 2 (FGF-2) and GDNF can promote the long-term survival of target-deprived adult mouse spiral ganglion neurons (Wei et al., 2007). Furthermore, GDNF was shown to contribute to synaptic development and maturation in ventral midbrain dopaminergic neurons and spinal cord motoneurons (Bourque and Trudeau, 2000). Therefore, conditional deletion of *Ret*, the canonical GDNF receptor, may affect retinal development and cause morphological and physiological alterations in *Chx10-Cre;C-Ret^{lox/lox}* mouse retinas.

Our study has documented dendritic sprouting in aging *Ret*-deficient mouse retinas. The outgrowth of bipolar cell dendrites was reported to be observed under some pathologic conditions, such as retinal detachment (Fisher et al., 2005), the *nob2* mouse with a calcium channel *Cav1.4* null mutation (Bayley and Morgans, 2007) and *Bsn* mice lacking functional Bassoon protein (Dick et al., 2003). A study of the RCS rat whose retina underwent progressive photoreceptor degeneration also demonstrated dendritic sprouting of rod bipolar cells (Cuenca et al., 2005). Furthermore, *NRTN*-deficient mice—a model deficit in one of GDNF family ligands—also showed abnormally located synapses in the ONL (Brantley et al., 2008). This study also suggested that the abnormal synapse formation in the ONL

caused deficits in the signaling of photoreceptor to bipolar cell and contributed to the ERG defects which was similar to what we have observed at 2–24 month of *Chx10-Cre;C-Ret^{lox/lox}* mice. However, a previous study indicated that the dendrites of rod bipolar cells, normally confined to the OPL, were found to extend into the ONL in normal aging retina and tended to increase in length and incidence with the age (Liets et al., 2006). Although the effect of aging could not be excluded in the abnormal synaptic formation of the *Ret*-deficient retina, the results of our ERG recordings, comparing *C-Ret^{lox/lox}* and *Chx10-Cre;C-Ret^{lox/lox}* mice at the age of 12 months, indicated that the *Chx10-Cre;C-Ret^{lox/lox}* mice may have dysfunctional bipolar cells. Additionally, a previous study speculated that reduced synaptic efficacy may induce new neuronal growth and the formation of ectopic synapses in *Basson* mutant mice (Dick et al., 2003). Therefore, combining our ERG and morphological results, we deduced that inadequate *Ret* expression may increase the formation of ectopic synapses and exacerbate these to a dysfunctional level. While not evaluated here, further studies should look to investigate the specific molecular mechanisms mediating the genesis and function of ectopic synapses in *Ret*-deficient mice.

CONCLUSION

In conclusion, our results provide evidence of the role of *Ret* in retinal development, which is essential to maintain the processes of horizontal cells and preserve the integrity of the OPL by stabilizing the structure of the synaptic ribbons. The *Chx10-Cre;C-Ret^{lox/lox}* mice developed in this study provided a valuable model in which to study *Ret* function in the retina and enhanced the understanding of *Ret* function in postnatal development and later stages. Finally, these conditional *Ret*-knockout mice might be useful for investigating the importance of GFL-mediated RET

activation in the retina of animal models of other diseases, such as neurodegenerative diseases or genetic disorders.

DATA AVAILABILITY STATEMENT

The raw data supporting the conclusions of this article will be made available by the authors, without undue reservation.

ETHICS STATEMENT

The animal study was reviewed and approved by the National Taiwan University Animal Ethics Committee.

AUTHOR CONTRIBUTIONS

W-HP conceived of the study, carried out the ultrastructure observation, drafted the manuscript, and final approval of the manuscript submission. M-LL participated in the design of the experiment and edited the manuscript. W-CH and C-YL carried out the antibody sensitivity test, immunohistochemical staining, and PCR experiment. SL edited the manuscript. Y-JT contributed with the electroretinography and data analysis. L-KY and K-JC contributed with the data analysis and interpretation. C-LC and N-KW designed the study, revised the work critically for important intellectual content, and gave their final approval of the version to be published. All the authors contributed to and approved the final manuscript.

FUNDING

This research was supported by grants to C-LC (106-2312-B-002-003 and 105-2320-B-002-008-MY3) from the Ministry of Science and Technology, Taiwan; a grant to W-HP (Isu-108-01-16A) from I-Shou University; grants to N-KW (NSC 102-2314-B-182-102-MY3) between 2013 and 2016 from the Ministry of Science and Technology, Taiwan; Vagelos College of Physicians & Surgeons Grants Program to N-KW from Columbia University

REFERENCES

- Airaksinen, M. S., and Saarma, M. (2002). The GDNF family: signalling, biological functions and therapeutic value. *Nat. Rev. Neurosci.* 3, 383–394. doi: 10.1038/nrn812
- Bayley, P. R., and Morgans, C. W. (2007). Rod bipolar cells and horizontal cells form displaced synaptic contacts with rods in the outer nuclear layer of the nob2 retina. *J. Comp. Neurol.* 500, 286–298. doi: 10.1002/cne.21188
- Berger, A., Cavallero, S., Dominguez, E., Barbe, P., Simonutti, M., Sahel, J.-A., et al. (2014). Spectral-domain optical coherence tomography of the rodent eye: highlighting layers of the outer retina using signal averaging and comparison with histology. *PLoS One* 9:e96494. doi: 10.1371/journal.pone.0096494
- Bourque, M. J., and Trudeau, L. E. (2000). GDNF enhances the synaptic efficacy of dopaminergic neurons in culture. *Eur. J. Neurosci.* 12, 3172–3180. doi: 10.1046/j.1460-9568.2000.00219.x

Irving Medical Center, grants from National Eye Institute to N-KW (R01EY031354) and to Core Support for Vision Research (5P30EY019007). The content is solely the responsibility of the authors and does not necessarily represent the official views of the National Institutes of Health.

ACKNOWLEDGMENTS

We thank the staff of the imaging core at the First Core Labs, National Taiwan University College of Medicine, for technical assistance. We would also like to acknowledge Dr. Rüdiger Klein, director and scientific member at the Max Planck Institute of Neurobiology, for kindly providing the *Ret^{Ret < tm1.1Kln >}* mice.

SUPPLEMENTARY MATERIAL

The Supplementary Material for this article can be found online at: <https://www.frontiersin.org/articles/10.3389/fnins.2021.728905/full#supplementary-material>

Supplementary Figure 1 | Calbindin staining of horizontal cells in *C-Ret^{dx/tx}* and *Chx10-Cre;C-Ret^{dx/tx}* retinas. Immunostaining against calbindin (green), a specific marker for horizontal cells, followed by counterstaining with Hoechst dye to indicate cell nuclei (blue) is shown. Compared to those of *C-Ret^{dx/tx}* mice (**A–D**), confocal microscopic images of horizontal cells at 2 month (**E**), 4 months (**F**), 12 months (**G**), and 24 months (**H**) of *Chx10-Cre;C-Ret^{dx/tx}* mice displayed a progressed decrease in calbindin-positive immunoreactivity with an increase in age. ONL, outer nuclear layer; OPL, outer plexiform layer; INL, inner nuclear layer; IPL, inner plexiform layer; GCL, ganglion cell layer. Scale bar, 25 μ m.

Supplementary Figure 2 | Mislocalization of photoreceptor synaptic terminals observed in *Chx10-Cre;C-Ret^{dx/tx}* mice. Retinal sections of animals aged 2, 4, 12, and 24 months were immunostained with an anti-PKC- α antibody (green) and an anti-PSD95 antibody (red), to label rod bipolar cells and the synapses of photoreceptors, respectively, followed by counterstaining with Hoechst dye, to indicate cell nuclei (blue) (**A–H**). The processes of rod bipolar cells formed synapses with photoreceptors in the OPL of *C-Ret^{dx/tx}* mice at all ages (**A–D**) and *Chx10-Cre;C-Ret^{dx/tx}* mice at the ages of 2 and 4 months (**E–F**). However, extended rod bipolar cell dendrites and ectopic photoreceptor terminals (arrows) in the ONL were observed in 12- and 24-month-old *Chx10-Cre;C-Ret^{dx/tx}* mice (**G,H**). ONL, outer nuclear layer; OPL, outer plexiform layer; INL, inner nuclear layer. Scale bar, 10 μ m.

- Brantley, M. A. Jr., Jain, S., Barr, E. E., Johnson, E. M. Jr., and Milbrandt, J. (2008). Neurturin-mediated ret activation is required for retinal function. *J. Neurosci.* 28, 4123–4135. doi: 10.1523/JNEUROSCI.0249-08.2008
- Chien, C. L., and Liem, R. K. (1995). The neuronal intermediate filament, alpha-internexin is transiently expressed in amacrine cells in the developing mouse retina. *Exp. Eye Res.* 61, 749–756. doi: 10.1016/s0014-4835(05)80026-0
- Chinskey, N. D., Besirli, C. G., and Zacks, D. N. (2014). Retinal cell death and current strategies in retinal neuroprotection. *Curr. Opin. Ophthalmol.* 25, 228–233. doi: 10.1097/ICU.0000000000000043
- Costantini, F., and Shakya, R. (2006). GDNF/Ret signaling and the development of the kidney. *Bioessays* 28, 117–127. doi: 10.1002/bies.20357
- Cuenca, N., Pinilla, I., Sauvé, Y., and Lund, R. (2005). Early changes in synaptic connectivity following progressive photoreceptor degeneration in RCS rats. *Eur. J. Neurosci.* 22, 1057–1072. doi: 10.1111/j.1460-9568.2005.04300.x

- Dick, O., Tom Dieck, S., Altmann, W. D., Ammermüller, J., Weiler, R., Garner, C. C., et al. (2003). The presynaptic active zone protein bassoon is essential for photoreceptor ribbon synapse formation in the retina. *Neuron* 37, 775–786. doi: 10.1016/s0896-6273(03)00086-2
- Durbec, P., Marcos-Gutierrez, C. V., Kilkenny, C., Grigoriou, M., Wartiowaara, K., Suvanto, P., et al. (1996). GDNF signalling through the Ret receptor tyrosine kinase. *Nature* 381, 789–793. doi: 10.1038/381789a0
- Ernsberger, U. (2008). The role of GDNF family ligand signalling in the differentiation of sympathetic and dorsal root ganglion neurons. *Cell Tissue Res.* 333, 353–371. doi: 10.1007/s00441-008-0634-4
- Errijgers, V., Van Dam, D., Gantois, I., Van Ginneken, C. J., Grossman, A. W., D'Hooge, R., et al. (2007). FVB.129P2-Pde6b(+) Tyr(c-ch)/Ant, a sighted variant of the FVB/N mouse strain suitable for behavioral analysis. *Genes Brain Behav.* 6, 552–557. doi: 10.1111/j.1601-183X.2006.00282.x
- Fisher, S. K., Lewis, G. P., Linberg, K. A., and Verardo, M. R. (2005). Cellular remodeling in mammalian retina: results from studies of experimental retinal detachment. *Prog. Retin. Eye Res.* 24, 395–431. doi: 10.1016/j.preteyeres.2004.10.004
- Frasson, M., Picaud, S., Leveillard, T., Simonutti, M., Mohand-Said, S., Dreyfus, H., et al. (1999). Glial cell line-derived neurotrophic factor induces histologic and functional protection of rod photoreceptors in the rd/rd mouse. *Investig. Ophthalmol. Vis. Sci.* 40, 2724–2734.
- Gabriel, R., Lesauter, J., Silver, R., Garcia-Espana, A., and Witkovsky, P. (2001). Diurnal and circadian variation of protein kinase C immunoreactivity in the rat retina. *J. Comp. Neurol.* 439, 140–150. doi: 10.1002/cne.1338
- Goetze, B., Schmidt, K. F., Lehmann, K., Altmann, W. D., Gundelfinger, E. D., and Lowel, S. (2010). Vision and visual cortical maps in mice with a photoreceptor synaptopathy: reduced but robust visual capabilities in the absence of synaptic ribbons. *Neuroimage* 49, 1622–1631. doi: 10.1016/j.neuroimage.2009.10.019
- Heidelberg, R., Thoreson, W. B., and Witkovsky, P. (2005). Synaptic transmission at retinal ribbon synapses. *Prog. Retin. Eye Res.* 24, 682–720. doi: 10.1016/j.preteyeres.2005.04.002
- Henderson, C. E. (1996). Role of neurotrophic factors in neuronal development. *Curr. Opin. Neurobiol.* 6, 64–70. doi: 10.1016/s0959-4388(96)80010-9
- Henderson, C. E., Phillips, H. S., Pollock, R. A., Davies, A. M., Lemeulle, C., Armanini, M., et al. (1994). GDNF: a potent survival factor for motoneurons present in peripheral nerve and muscle. *Science (New York, NY)* 266, 1062–1064. doi: 10.1126/science.7973664
- Johnson, T. V., Bull, N. D., and Martin, K. R. (2011). Neurotrophic factor delivery as a protective treatment for glaucoma. *Exp. Eye Res.* 93, 196–203. doi: 10.1016/j.exer.2010.05.016
- Koeberle, P. D., and Ball, A. K. (1998). Effects of GDNF on retinal ganglion cell survival following axotomy. *Vision Res.* 38, 1505–1515. doi: 10.1016/s0042-6989(97)00364-7
- Kramer, E. R., Aron, L., Ramakers, G. M., Seitz, S., Zhuang, X., Beyer, K., et al. (2007). Absence of Ret signaling in mice causes progressive and late degeneration of the nigrostriatal system. *PLoS Biol.* 5:e39. doi: 10.1371/journal.pbio.0050039
- Kramer, E. R., Knott, L., Su, F., Dessaud, E., Krull, C. E., Helmbacher, F., et al. (2006). Cooperation between GDNF/Ret and ephrinA/EphA4 signals for motor-axon pathway selection in the limb. *Neuron* 50, 35–47. doi: 10.1016/j.neuron.2006.02.020
- Lenzi, D., and von Gersdorff, H. (2001). Structure suggests function: the case for synaptic ribbons as exocytotic nanomachines. *Bioessays* 23, 831–840. doi: 10.1002/bies.1118
- Liets, L. C., Eliasieh, K., van der List, D. A., and Chalupa, L. M. (2006). Dendrites of rod bipolar cells sprout in normal aging retina. *Proc. Natl. Acad. Sci. U.S.A.* 103:12156. doi: 10.1073/pnas.0605211103
- Lin, L. F., Doherty, D. H., Lile, J. D., Bektesh, S., and Collins, F. (1993). GDNF: a glial cell line-derived neurotrophic factor for midbrain dopaminergic neurons. *Science (New York, NY)* 260, 1130–1132. doi: 10.1126/science.8493557
- LoGiudice, L., and Matthews, G. (2009). The role of ribbons at sensory synapses. *Neuroscientist* 15, 380–391. doi: 10.1177/107385840831373
- Mattapallil, M. J., Wawrousek, E. F., Chan, C. C., Zhao, H., Roychowdhury, J., Ferguson, T. A., et al. (2012). The Rd8 mutation of the Crbl1 gene is present in vendor lines of C57BL/6N mice and embryonic stem cells, and confounds ocular induced mutant phenotypes. *Invest. Ophthalmol. Vis. Sci.* 53, 2921–2927. doi: 10.1167/iovs.12-9662
- Mead, B., Thompson, A., Scheven, B. A., Logan, A., Berry, M., and Leadbeater, W. (2014). Comparative evaluation of methods for estimating retinal ganglion cell loss in retinal sections and wholemounts. *PLoS One* 9:e110612. doi: 10.1371/journal.pone.0110612
- Meng, X., Lindahl, M., Hyvonen, M. E., Parvinen, M., de Rooij, D. G., Hess, M. W., et al. (2000). Regulation of cell fate decision of undifferentiated spermatogonia by GDNF. *Science (New York, NY)* 287, 1489–1493. doi: 10.1126/science.287.5457.1489
- Moore, M. W., Klein, R. D., Farinas, I., Sauer, H., Armanini, M., Phillips, H., et al. (1996). Renal and neuronal abnormalities in mice lacking GDNF. *Nature* 382, 76–79. doi: 10.1038/382076a0
- Nag, T. C., and Wadhwa, S. (2001). Differential expression of syntaxin-1 and synaptophysin in the developing and adult human retina. *J. Biosci.* 26, 179–191. doi: 10.1007/BF02703642
- Ogilvie, J. M., Speck, J. D., and Lett, J. M. (2000). Growth factors in combination, but not individually, rescue rd mouse photoreceptors in organ culture. *Exp. Neurol.* 161, 676–685. doi: 10.1006/exnr.1999.7291
- Popsueva, A., Poteryaev, D., Arighi, E., Meng, X., Angers-Loustau, A., Kaplan, D., et al. (2003). GDNF promotes tubulogenesis of GFRalpha1-expressing MDCK cells by Src-mediated phosphorylation of Met receptor tyrosine kinase. *J. Cell. Biol.* 161, 119–129. doi: 10.1083/jcb.200212174
- Rothermel, A., and Layer, P. G. (2003). GDNF regulates chicken rod photoreceptor development and survival in reaggregated histotypic retinal spheres. *Invest. Ophthalmol. Vis. Sci.* 44, 2221–2228. doi: 10.1167/iovs.02-0915
- Rothermel, A., Volpert, K., Burghardt, M., Lantsch, C., Robitzki, A. A., and Layer, P. G. (2006). Knock-down of GFRalpha4 expression by RNA interference affects the development of retinal cell types in three-dimensional histotypic retinal spheres. *Invest. Ophthalmol. Vis. Sci.* 47, 2716–2725. doi: 10.1167/iovs.05-1472
- Rowan, S., and Cepko, C. L. (2004). Genetic analysis of the homeodomain transcription factor Chx10 in the retina using a novel multifunctional BAC transgenic mouse reporter. *Dev. Biol.* 271, 388–402. doi: 10.1016/j.ydbio.2004.03.039
- Sariola, H., and Saarna, M. (2003). Novel functions and signalling pathways for GDNF. *J. Cell. Sci.* 116(Pt 19), 3855–3862. doi: 10.1242/jcs.00786
- Schuchardt, A., D'Agati, V., Larsson-Blomberg, L., Costantini, F., and Pachnis, V. (1994). Defects in the kidney and enteric nervous system of mice lacking the tyrosine kinase receptor Ret. *Nature* 367, 380–383. doi: 10.1038/367380a0
- Sterling, P., and Matthews, G. (2005). Structure and function of ribbon synapses. *Trends Neurosci.* 28, 20–29. doi: 10.1016/j.tins.2004.11.009
- Takahashi, M. (2001). The GDNF/RET signaling pathway and human diseases. *Cytokine Growth Factor Rev.* 12, 361–373. doi: 10.1016/s1359-6101(01)00012-0
- Wang, N. K., Tosi, J., Kasanuki, J. M., Chou, C. L., Kong, J., Parmalee, N., et al. (2010). Transplantation of reprogrammed embryonic stem cells improves visual function in a mouse model for retinitis pigmentosa. *Transplantation* 89, 911–919. doi: 10.1097/TP.0b013e3181d45a61
- Wei, D., Jin, Z., Jarlebark, L., Scarfone, E., and Ulfendahl, M. (2007). Survival, synaptogenesis, and regeneration of adult mouse spiral ganglion neurons in vitro. *Dev. Neurobiol.* 67, 108–122. doi: 10.1002/dneu.20336
- Will, E., Klump, H., Heffner, N., Schwieger, M., Schiedmeier, B., Ostertag, W., et al. (2002). Unmodified Cre recombinase crosses the membrane. *Nucleic Acids Res.* 30, e59. doi: 10.1093/nar/gnf059

- Wu, W. C., Lai, C. C., Chen, S. L., Sun, M. H., Xiao, X., Chen, T. L., et al. (2004). GDNF gene therapy attenuates retinal ischemic injuries in rats. *Mol. Vis.* 10, 93–102.
- Yan, Q., Wang, J., Matheson, C. R., and Urich, J. L. (1999). Glial cell line-derived neurotrophic factor (GDNF) promotes the survival of axotomized retinal ganglion cells in adult rats: comparison to and combination with brain-derived neurotrophic factor (BDNF). *J. Neurobiol.* 38, 382–390. doi: 10.1002/(sici)1097-4695(19990215)38:3<382::aid-neu7<3.0.co;2-5

Conflict of Interest: The authors declare that the research was conducted in the absence of any commercial or financial relationships that could be construed as a potential conflict of interest.

Publisher's Note: All claims expressed in this article are solely those of the authors and do not necessarily represent those of their affiliated organizations, or those of the publisher, the editors and the reviewers. Any product that may be evaluated in this article, or claim that may be made by its manufacturer, is not guaranteed or endorsed by the publisher.

Copyright © 2021 Peng, Liao, Huang, Liu, Levi, Tseng, Lee, Yeh, Chen, Chien and Wang. This is an open-access article distributed under the terms of the Creative Commons Attribution License (CC BY). The use, distribution or reproduction in other forums is permitted, provided the original author(s) and the copyright owner(s) are credited and that the original publication in this journal is cited, in accordance with accepted academic practice. No use, distribution or reproduction is permitted which does not comply with these terms.